

## Methods for the Study of Clustering and Precipitation in Al-based Alloys by APT

Williams Lefebvre<sup>1</sup>, François Vurpillot<sup>1</sup>, Malin Torsaeter<sup>2</sup>, Frédéric De Geuser<sup>3</sup>

<sup>1</sup>Groupe de Physique des Matériaux, CNRS – UMR 6634, Saint-Etienne du Rouvray, France

<sup>2</sup>Norwegian University of Science and Technology NTNU, Department of Physics, Høgskoleringen  
5, N-7491 Trondheim, Norway

<sup>3</sup>SIMaP, Grenoble INP, CNRS, UJF, 1130 Rue de la Piscine BP 75 38 402 St Martin d'Hères Cedex, France

Clusters formed during natural ageing, pre-ageing or artificial ageing are known to play a critical role in the precipitation sequence of some age hardenable Al-based alloys. The determination of their nature, size and number density is of crucial importance if one needs to understand their influence of the later formation of hardening phases. Atom Probe Tomography (APT) is the unique technique enabling the direct observation of solute clustering at the atomic scale. However, a quantitative analysis of clustering is not straight forward and has been the subject of continuous efforts for the development of new tools in the APT community. In the present work, we present original approaches dedicated to the study of clustering.

**Keywords:** *clustering, atom probe tomography*

### 1. Introduction

Atom probe tomography (APT), which is based on reconstruction of a small volume of a sharp tip evaporated by field effect, has unique capabilities to characterize materials (metals, alloys, oxides, thin multilayer films on planar substrates, dielectric films, semiconducting structures and devices, and ceramic materials). Indeed, APT delivers the highest spatial resolution (sub-0.3-nm) three-dimensional compositional information of any microscopy technique. Usual data provided by APT are 3D reconstructions wherein roughly half of the atoms (this quantity is related to the average detection efficiency of standard atom probes) are displayed with a near lattice resolution. From 3D reconstructions, a large amount of information can be extracted (like concentration profiles, phase composition, radial distribution of elements...) thanks to the availability of both chemical nature of elements and the (x,y,z) coordinates of each atom in the volume.

APT has been widely and successfully used for the characterization of precipitation in Al-based alloys. However, it is clear that the study of clustering by APT, which is a major issue in Al-based alloys, is not straight forward and requires very specific approaches. For instance, the clusters formed during natural ageing, pre-ageing or artificial ageing are known to play a critical role in the precipitation sequence of some age hardenable Al-based alloys [1]. The determination of their nature, size and number density is of crucial importance if one needs to understand their influence of the later formation of hardening phases. Nevertheless, the available algorithms for cluster identification in APT data sets [2-6] may rapidly lead to unrealistic results if they are not well used or may simply fail in analysing clusters smaller than a critical size. In this work, we have chosen to apply existing and original methods to a model data set of an Al-based alloy (model A-0.7at%B simulated data) containing a fine dispersion of small clusters (9 solute atoms in average). By evaluating the influence of cluster search parameters on output data and by using an original approach for the determination of cluster concentration, we propose a new methodology for the characterization of clustering in Al-based alloys by Atom Probe Tomography;

### 2. Basic procedure for simulation of clusters in APT data sets

To realistically reflect the influence of the instrument transfer function on the atomic positions, we have chosen to use a real APT dataset as a basis for the simulated volumes. Each atom has then be re-labelled to a chosen chemical element so that the dataset satisfied a given set of clusters of given concentration and size. An analysis of volume  $V = 20 \text{ nm} \times 30 \text{ nm} \times 30 \text{ nm}$  containing roughly 800 000 atoms was chosen. The simulated volume contains atoms of solvent A and atoms of solute B. The concentration of B atoms within clusters is set to 25at% whereas it is 0.7 at% in the matrix. Such parameters correspond to what is observed in the Al-Mg-Si system for instance. Rather than using a complex procedure involving the short range order parameter, as done by L.T. Stephenson [7], we have attributed an ellipsoidal shape to clusters. The sizes of axes  $a$ ,  $b$  and  $c$  axes for the ellipsoids were randomly chosen in the respective ranges 0.6-1.2 nm, 0.8-1.6 nm and 1.8-2.4 nm. Pictures showing the simulated APT data sets are given in Fig. 1. General information about the input data of the simulated data set are given in Table 1 at the end of this paper.

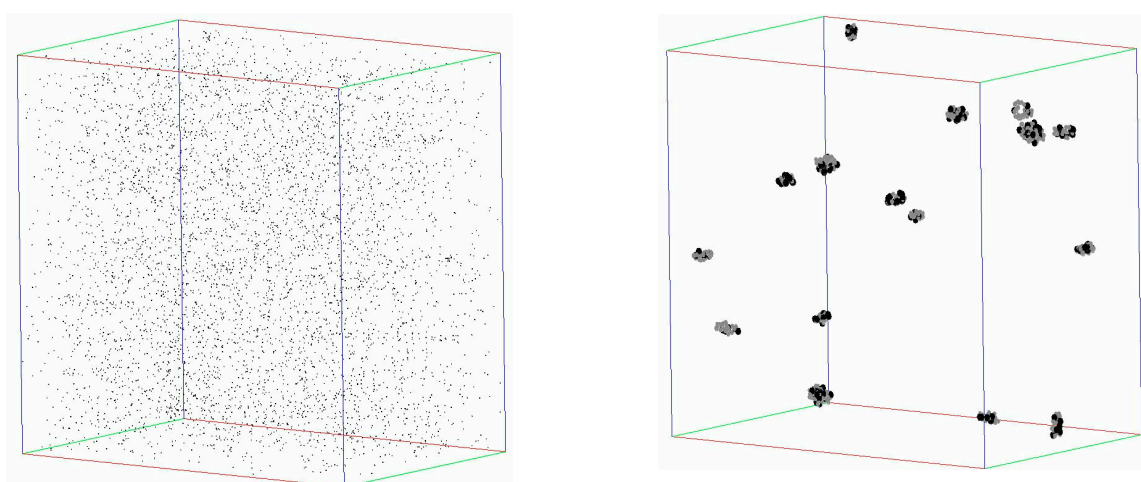


Figure 1: On the left, distribution of solute atoms in the simulated APT data set (concentration in the matrix of 0.7at% and 25at% in clusters) and, on the right, only solute rich clusters are displayed. Solute atoms are displayed in black whereas solvent atoms are in grey. The volume is  $20 \times 30 \times 30 \text{ nm}^3$

### 3. Results

From the rough pictures including only solute atoms in Fig.1, it is clear that solute clustering is absolutely not obvious by eye. This is actually often the case when solute segregation is considered. There are roughly two ways to give evidence of clustering. The first way consists in applying some statistical treatment to the reconstruction (like radial distribution function, pair correlation, frequency distribution of concentration, nearest neighbours distances). A second way consists in showing clusters with help of a cluster identification algorithm. Though several algorithms have been developed, the most common one method used is based on the maximum separation distance (MSD) [2] between solutes. The MSD algorithm works as follows. It defines solute atoms with a separation smaller than a distance  $d_{\max}$  as belonging to one single cluster. Clusters containing less than a certain minimum number of atoms ( $N_{\min}$ ) are taken to be the result of random fluctuations and ignored. Since it is based on nearest neighbour distances, the maximum separation method is a localized algorithm well suited to study fine-scaled clustering of dilute solute alloys. In his PhD thesis [7] and in the reference [6], L.T. Stephenson and his co-workers presented a very detailed investigation of the clustering as studied by APT. For instance, they paid much attention to the influence of the parameters  $N_{\min}$  and  $d_{\max}$  for the further extraction of data related to cluster. They also proposed an improved algorithm designated as “core-linkage” which is detailed in the following reference [6].

In the present work, we focus first on the possibility to extract reliable clustering information based on the MSD algorithm, thanks to simulations and heuristic determination of input parameters

$N_{\min}$  and  $d_{\max}$ . Then, we propose an original approach for the association of other elements (like other addition elements of the solvent) to the solute-rich cluster.

### 3.1 First nearest neighbour distance analysis

By plotting first nearest neighbours (1NN) distances (see reference [8] for instance), one can get a direct indication of the clustering or precipitation stage in an alloy. Since the MSD algorithm is directly based on 1NN distances, it is mandatory to plot the 1NN distribution before the MSD method is applied. In Fig. 2, the 1NN distance distributions are plotted for two simulated APT reconstructions of identical size: a volume of matrix with about 0.7at% of solute and the volume shown in Fig. 1.

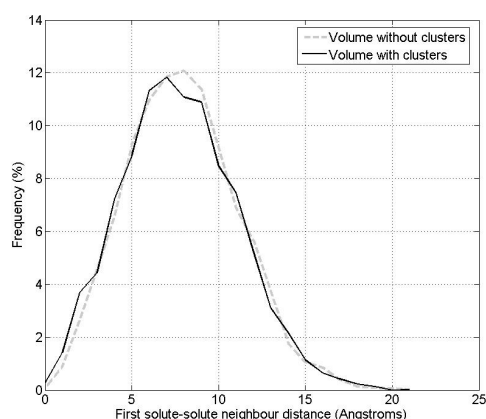


Figure 2: 1NN distance distribution in two simulated APT reconstructions of size  $20 \times 30 \times 30 \text{ nm}^3$ . Both volumes contain 788978 atoms. The volume without clusters is simulated matrix with random distribution of B atoms (concentration 0.7at%) in a solvent A. The volume with clusters is the one shown in Fig. 1.

From Fig.2, it is visible that no clear difference is observed between the volume containing clusters and the one without any cluster. This is due to the fact that, in the volume with clusters, most of the signal is generated by solute atoms in the matrix (5300 vs 170 in clusters). Hereafter, the volume without clusters will be used as a reference. Indeed, it is very well known that the MSD algorithm generates some “noise” since clusters may artificially be observed in a volume where solute are randomly distributed. Hence, the MSD will be applied in both volumes (i.e. with and without clusters) and results will be compared.

### 3.2 Amount of clusters detected by the MSD algorithm as a function of input parameters.

We have applied the MSD algorithm in both volumes (i.e. with and without clusters) and we have counted the amount of clusters detected as a function of input parameters  $N_{\min}$  and  $d_{\max}$ . Results are shown in Fig. 3 and 4. One has to keep in mind that the actual amount of clusters in the volume is 18 (see Table 1) and that some of these clusters contain very few solute atoms. Hence, the very large amount of clusters found for large  $d_{\max}$  (10 Å) and low  $N_{\min}$  (<4) is unrealistic since it is produced by solute atoms in the matrix. In Fig. 4, we calculated a ratio between the amount clusters detected by MSD (as function of input parameters  $d_{\max}$  and  $N_{\min}$ ) in the volume without clusters and the volume with clusters. A ratio close to 1 or larger than 1 indicates that the set of parameters generates more noise than signal from real clusters. On the opposite, a ratio much less than 1 indicates that the clusters detected by the MSD algorithm are more likely to be produced by real clusters.

In order to choose a reliable set of parameters, both data provided by Fig. 3 and 4 must be considered. In the present illustration, a  $d_{\max}$  close to 6-7 Å and a value of  $N_{\min}$  close to 6 give both a low noise level (i.e. few artificial clusters) and a realistic amount of clusters.

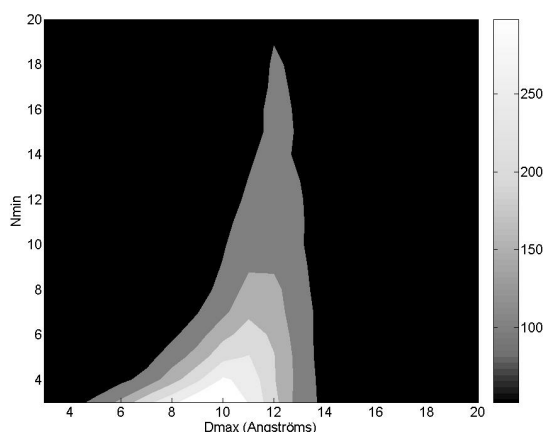


Figure 3: Amount of clusters detected by MSD in the volume containing clusters, as function of input parameters  $d_{\max}$  and  $N_{\min}$ . The scale is displayed on the right.

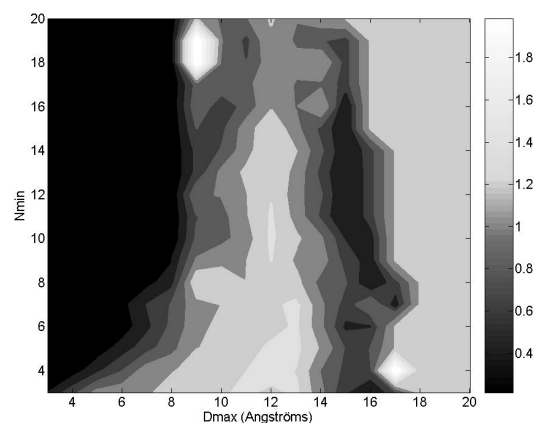


Figure 4: Ratio between the amount clusters detected by MSD (as function of input parameters  $d_{\max}$  and  $N_{\min}$ ) in the volume without clusters and the volume with clusters. Areas in black correspond to reliable parameters (i.e. larger signal over noise ratio).

### 3.3 Original method (LCM) for the association of other atoms to solute-rich clusters

The use of the MSD algorithm is not sufficient to characterize clustering. Indeed, if an alloy contains B, C and D solute atoms and a solvent A, if the MSD is applied for B atoms only, it is necessary to determine how many A, C and D atoms belong to a given cluster. This might be done with the envelope method [3]. However, this method is based on the use of a grid (which steps have to be defined) and provides a strong roughness together with a cuboidal shape to clusters. Moreover, it becomes totally uncertain when solute clusters are not dense or contain very few atoms (typically less than 10). Other methods exist that need the definition of a distance for the association of other species [3, 6]. Once again, the definition of this distance is not obvious. Here, we propose an original way to associate other atoms to an identified solute-rich cluster. This method, referred to as LCM (for local centre of mass).

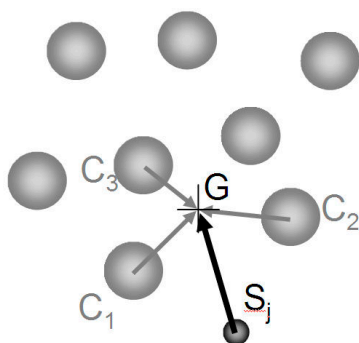


Figure 5: Schematic description of the LCM method for association of other elements to a cluster. Large grey atoms are solute atoms already identified as belonging to a same cluster.  $S_j$  is an atom which might belong to the cluster.  $C_1$ ,  $C_2$  and  $C_3$  are the 3 first neighbour cluster atoms of the atom  $S_j$ .  $G$  is the centre of mass of atoms cluster atoms  $C_1$ ,  $C_2$  and  $C_3$ .

Before the LCM method is applied to a cluster, the  $N$  solute atoms  $C_i$  of the cluster must be identified (by MSD for instance). Then, for any other atom  $S_j$  in the vicinity of the cluster, the  $M$   $C_i$  atoms closer to  $S_j$  are identified. Then the local centre of mass  $G$  of the  $M$   $C_i$  atoms is calculated. The  $S_j$  atom is associated to the cluster if at least one of the  $C_iG$  distances is larger than the  $S_jG$  distance.

### 3.4 Combination of the LCM and MSD methods for the study of clustering in the simulated APT data set.

We have applied the MSD ( $N_{\min} = 6$  and  $d_{\max} = 6.5$  Å) and LCM ( $M=3$ ) algorithms to the same

simulated volume containing clusters displayed in Fig.1. Results are summarized in Table 1 and they are directly compared to the input data of the simulated volume. Results are also directly visible in Figure 6. For the set of parameters  $N_{\min} = 6$  and  $d_{\max} = 6.5 \text{ \AA}$  deduced from Fig. 3 and 4, there is an excellent agreement for both the number density of clusters in the volume and the average amount of solute atoms per clusters. As for the LCM method applied with  $M=3$  for the amount of cluster atom neighbours, it provides a very satisfying value for the average concentration of solutes in clusters (20.1 vs 22.0 in the input data). Values of standard deviation are not given here since they reflect more the large distribution of the input data rather than a measurement of the error introduced by the methodology of cluster identification.

**Table 1.** On the left of the table, the input information about solute clusters in the simulated APT reconstruction containing clusters is given. The right part of the table contains the data obtained by applying the combination of MSD ( $N_{\min} = 6$  and  $d_{\max} = 6.5 \text{ \AA}$ ) and LCM ( $M=3$ ) algorithms to the same volume.

Input data of the simulated volume					Data obtained after application of MSD and LCM to the simulated volume				
Cluster number	Amount of atoms			Solute concentration (at.%)	Cluster number	Amount of atoms			Solute concentration (at.%)
	solute	solvent	total			solute	solvent	total	
1	3	31	34	8.9	1	14	29	43	32.6
2	5	37	42	11.9	2	7	19	26	26.9
3	13	56	69	18.8	3	6	15	21	28.6
4	6	28	34	17.6	4	15	58	73	20.5
5	14	40	54	25.9	5	6	36	42	14.3
6	20	69	89	22.5	6	15	55	70	21.4
7	10	21	31	32.3	7	6	31	37	16.2
8	6	21	27	22.2	8	12	95	107	11.2
9	11	23	34	32.4	9	13	38	51	25.5
10	15	48	63	23.8	10	9	39	48	18.8
11	12	20	32	37.5	11	14	34	48	29.2
12	13	36	49	26.5	12	6	34	40	15.0
13	9	33	42	21.4	13	7	19	26	26.9
14	5	33	38	13.2	14	8	90	98	8.2
15	8	24	32	25	15	21	100	121	17.4
16	5	34	39	12.8	16	8	79	87	9.2
17	11	30	41	26.8	-	-	-	-	-
18	4	20	24	16.7	-	-	-	-	-
Average	9.4	33.6	43.0	22.0		10.4	48.2	58.6	20.1

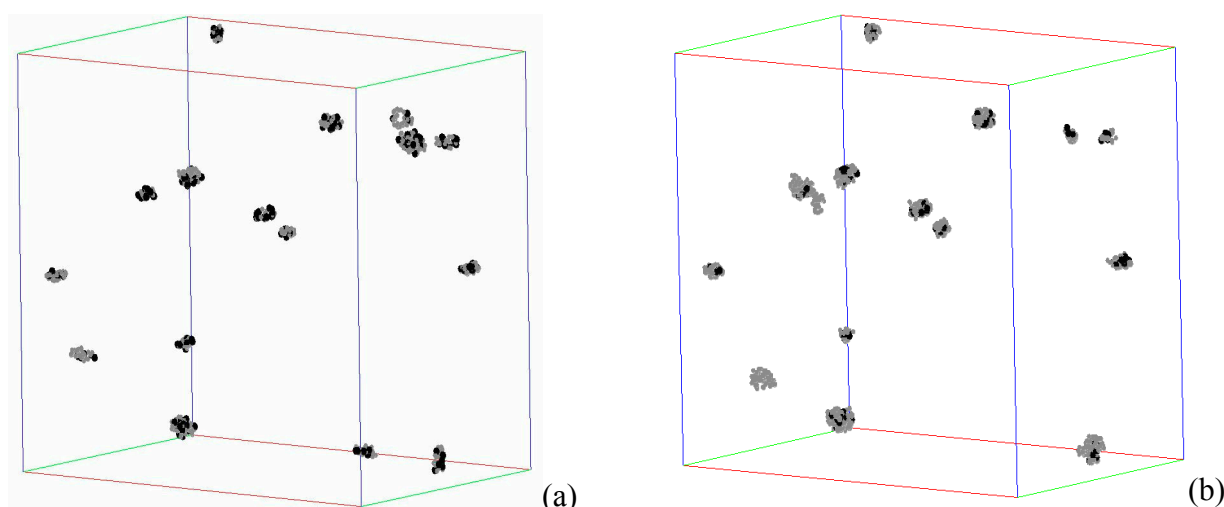


Figure 6: The APT volume is  $20 \times 30 \times 30 \text{ nm}^3$ . Solute atoms are black and atoms of the major element are grey. (a) Solute rich clusters as they were introduced in the simulated data set are shown. (b) Solute rich clusters identified using the combination of MSD ( $N_{\min} = 6$  and  $d_{\max} = 6.5 \text{ \AA}$ ) and LCM ( $M=3$ ) algorithms to the same volume as (a).

#### 4. Conclusion

We have shown that the study of clustering in Al-based alloys by atom probe tomography is not a trivial issue and may lead to unrealistic results if cluster identification algorithms are not used with a maximum of attention. In this paper, we propose a way to select input parameters of the maximum separation distance by comparing results obtained in the real APT data set with those obtained with its equivalent randomized data set. Reliable parameters are then chosen by finding a compromise of good signal over noise ratio and realistic amount of clusters. Then, we have presented an original method, that enables the reliable calculation of cluster concentration thanks to the association of all chemical elements to each cluster. We have demonstrated that this methodology enables the quantitative analysis of extremely small cluster (6 solute atoms) in a matrix containing 0.7 at% of a solute element.

#### References

- [1] D. W. Pashley, J. W. Rhodes and A. Sendorek: J. Inst. Met. 94, 41 (1966).
- [2] J.M. Hyde (1993). PhD dissertation. Oxford: University of Oxford.
- [3] M.K. Miller *Atom Probe Tomography*. New York: Kluwer Academic/ Plenum publishers. (2000)
- [4] D. Vaumousse, A. Cerezo, P.J. Warren: Ultramicroscopy 95 (2003) 215 – 221.
- [5] W. Lefebvre, G. Da Costa, F. De Geuser, A. Deschamps, F. Danoix: Surface and Interface Analysis 39 (2007) 206-212.
- [6] L.T. Stephenson, M.P. Moody, P.V. Liddicoat, S.P. Ringer : Microscopy and Microanalysis 13 (2007), 448–463.
- [7] L.T. Stephenson, PhD Dissertation: the University of Sydney (2010).
- [8] T. Philippe, F. De Geuser, S. Duguay, W. Lefebvre, O. Cojocar-Mirédin, G. Costa, D. Blavette: Ultramicroscopy 109 (2009) 1304-1309.